

# Impedance spectroscopy of $\text{Ba}_4\text{Ti}_{13}\text{O}_{30}$ film prepared by laser chemical vapor deposition

Dongyun Guo · Takashi Goto · Chuanbin Wang ·  
Qiang Shen · Lianmeng Zhang

Received: 29 September 2011 / Accepted: 7 March 2012 / Published online: 21 March 2012  
© Springer Science+Business Media, LLC 2012

**Abstract** The impedance and electrical conductivity of  $\text{Ba}_4\text{Ti}_{13}\text{O}_{30}$  film prepared by laser chemical vapor deposition were investigated as functions of temperature (300–1073 K) and frequency ( $10^2$ – $10^7$  Hz). The impedance response was resolved into two contributions, which were associated with the grains ( $R_g C_g$ ) and grain boundaries ( $R_{gb} C_{gb}$ ). With increasing temperature, both  $R$  and  $C$  decreased.  $R_{gb}$  was much higher than  $R_g$  and  $C_g$  were close to  $C_{gb}$ . Below 876 K, a step-like behavior was observed in the ac conductivity plots as functions of frequency due to two dispersion regions. The low-frequency dispersion was associated with grain boundaries and the high-frequency one corresponded to grains. The activation energies of grain conduction ( $E_g$ ) and grain boundary conduction ( $E_{gb}$ ) were 0.20 and 1.49 eV, respectively, which indicated that the relaxation process in grains arose from hopping electron and that in grain boundaries from the diffusion of oxygen vacancies.

**Keywords**  $\text{Ba}_4\text{Ti}_{13}\text{O}_{30}$  film · Laser chemical vapor deposition · Impedance · Electrical conductivity

## 1 Introduction

Compounds in the BaO– $\text{TiO}_2$  system have attracted great attention due to their excellent dielectric properties, which

can be applied to microwave devices [1–3]. Among them,  $\text{Ba}_4\text{Ti}_{13}\text{O}_{30}$  compound was firstly found in quenched samples prepared by the solid-state reaction, which was only used to improve microwave dielectric property of the other compounds as additive, since it was very difficult to obtain the single-phase  $\text{Ba}_4\text{Ti}_{13}\text{O}_{30}$  compound [4–6].

Recently, we reported on preparation of single-phase  $\text{Ba}_4\text{Ti}_{13}\text{O}_{30}$  film prepared by laser chemical vapor deposition (LCVD) [7]. The films prepared by LCVD had typically columnar cross-section. The presence of grain boundaries between the columnar grains could be one of the major factors to influence the electrical properties of these films. For application in microwave devices, it is necessary to understand the mechanisms of conduction and to determine the electrical behaviors of grains and grain boundaries in  $\text{Ba}_4\text{Ti}_{13}\text{O}_{30}$  film. Impedance spectroscopy is considered as a powerful technique to evaluate the relationship between microstructure and electrical properties and distinguish the intrinsic (grain) and extrinsic contributions (such as grain boundary, surface layer, electrode contact problem and impurity phase) [8]. This technique has been successfully applied to analyze the electrical properties of dielectric materials, such as  $\text{BaTiO}_3$ ,  $\text{LiTaO}_3$ ,  $\text{BiFeO}_3$  and  $\text{CaCu}_3\text{Ti}_4\text{O}_{12}$  [9–12]. In this study, we investigated the impedance, modulus and ac conductivity of  $\text{Ba}_4\text{Ti}_{13}\text{O}_{30}$  film prepared by LCVD as functions of temperature and frequency.

## 2 Experimental

The details of preparation of  $\text{Ba}_4\text{Ti}_{13}\text{O}_{30}$  film were reported elsewhere [7]. The thickness of  $\text{Ba}_4\text{Ti}_{13}\text{O}_{30}$  film was 14.9  $\mu\text{m}$ . To measure electrical properties, electrode was fabricated on the surface from Au paste, which was dried and decomposed by gradually heating to 1073 K. The area

D. Guo (✉) · C. Wang · Q. Shen · L. Zhang  
State Key Laboratory of Advanced Technology for Materials  
Synthesis and Processing, and School of Materials Science  
and Engineering, Wuhan University of Technology,  
Wuhan 430070, China  
e-mail: guodongyun@gmail.com

D. Guo · T. Goto  
Institute for Materials Research, Tohoku University,  
Sendai 980-8577, Japan

of Au electrode was about 0.9 mm<sup>2</sup>. Impedance spectroscopic measurements were performed using an impedance/grain-phase analyzer (Hewlett Packard 4194) in the temperature range from 300 to 1073 K over the frequency range of 10<sup>2</sup>–10<sup>7</sup> Hz.

### 3 Results and discussion

Figure 1 shows the Cole–Cole plots of complex impedance data (the imaginary part  $Z''$  and the real part  $Z'$ ) of Ba<sub>4</sub>Ti<sub>13</sub>O<sub>30</sub> film at different temperatures. The arrow in Fig. 1(a) showed the direction of increasing frequency. At low temperature, the almost straight line with big slope indicated that the film had high impedance. With increasing temperature, the impedance decreased and the semicircular arcs were observed above 723 K. There were two poorly resolved semicircular arcs in Fig. 1(b), which were attributed to the responses of grains (high frequency) and grain boundaries (low frequency), respectively. The small arc was largely obscured by the larger semicircular arc due to the large difference in the magnitudes of resistance between grain ( $R_g$ ) and grain boundary ( $R_{gb}$ ). The Cole–Cole plot in Fig. 1(c) showed a depressed semicircle due to grain boundary.

Since the semicircle sizes in Cole–Cole plots were coincided with the magnitude of resistance, if the two responses had greatly different magnitudes of  $R$  (often by orders of magnitude), the more resistive response dominated entirely making resolution of the less resistive response difficult. In this cases, modulus spectra was useful for resolving the different relaxations [13]. Figure 2 shows modulus spectra (the imaginary part  $M''$  and the real part  $M'$ ) of Ba<sub>4</sub>Ti<sub>13</sub>O<sub>30</sub> film. The arrow in Fig. 2 also showed the direction of increasing frequency. There were two arcs in the modulus spectra below 917 K, one at low frequency and another at high frequency, indicating the presence of two relaxations. An equivalent circuit comprising two parallel  $RC$  elements in series was supposed as shown in Fig. 2. The low-frequency arc corresponded to the grain boundary response ( $R_{gb}C_{gb}$ ) and the high-frequency arc corresponded to the grain response ( $R_gC_g$ ). The peak in the modulus spectra is described by

$$M'' = \frac{\varepsilon_0}{C} \left[ \frac{\omega RC}{1 + (\omega RC)^2} \right] \tag{1}$$

where  $\varepsilon_0$  is the permittivity of free space,  $\omega$  is the angular frequency and given by

$$\omega = 2\pi f \tag{2}$$

The frequency at the semicircular arc maxima ( $f_{max}$ ) for each  $RC$  element is given by

$$2\pi f_{max} RC = 1 \tag{3}$$

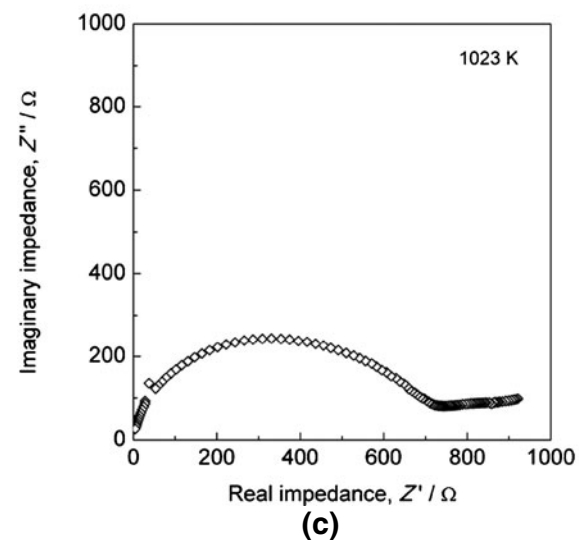
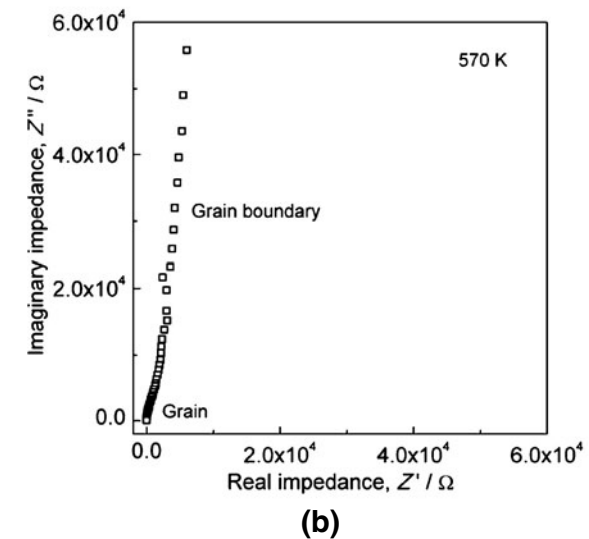
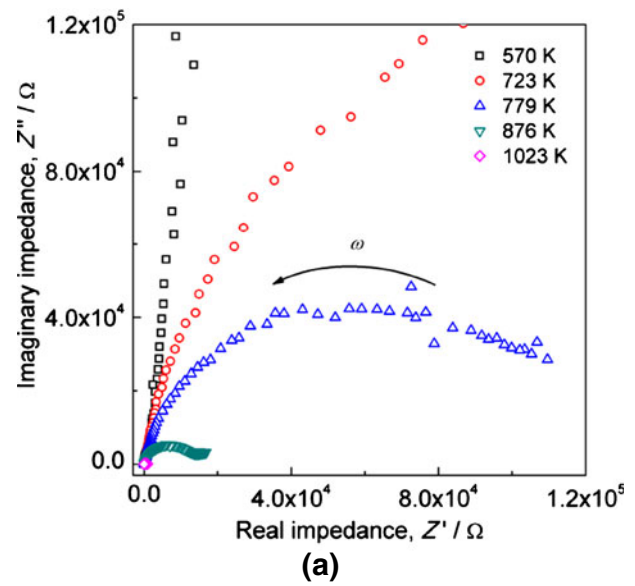
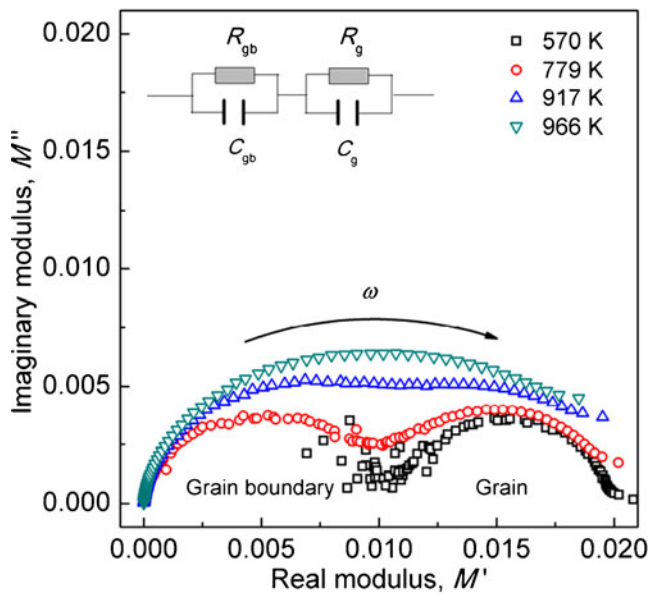


Fig. 1 Cole–Cole plots of Ba<sub>4</sub>Ti<sub>13</sub>O<sub>30</sub> film: (a) measured at different temperatures, (b) at 570 K and (c) at 1023 K



**Fig. 2** Modulus spectra of Ba<sub>4</sub>Ti<sub>13</sub>O<sub>30</sub> film measured at different temperatures, the inset shows an equivalent circuit comprising two parallel RC elements in series

From equations (1) and (3), the magnitude of  $M''_{max}$  at the peak maxima is given by

$$M''_{max} = \frac{\epsilon_0}{2C} \tag{4}$$

Hence, the magnitudes of  $R$  and  $C$  can be estimated from  $M''_{max}$  of the modulus spectra. According to Fig. 2, with increasing temperature,  $M''_{max}$  increased, which indicated both  $C_g$  and  $C_{gb}$  decreased, and the two semicircular arcs gradually merged together. When temperature was above 917 K, only one semicircular arc was observed. In order to analyze the change,  $M''$  as a function of frequency of Ba<sub>4</sub>Ti<sub>13</sub>O<sub>30</sub> film at different temperatures are plotted in Fig. 3. At 356 K, one peak labeled as peak I was observed at low frequency. With increasing temperature, the position of peak I ( $f_{maxI}$ ) shifted toward high frequency. At 570 K, another peak labeled as peak II appeared at low frequency. As temperature increased, the position of peak II ( $f_{maxII}$ ) also shifted toward high frequency just like peak I. Peak I was associated with  $R_g C_g$  and peak II was associated with  $R_{gb} C_{gb}$ . However, when temperature was above 779 K,  $f_{maxI}$  increased very slowly. With increasing temperature, the intensity of peak II increased rapidly. Above 966 K, peak II merged peak I, which indicated that the dominant contribution was from grain boundary. The values of  $R$  and  $C$  were calculated using equations (3) and (4), and listed in Table 1. With increasing temperature, both  $R$  and  $C$  decreased.  $C_g$  was close to  $C_{gb}$  and  $R_{gb}$  was much higher than  $R_g$ .

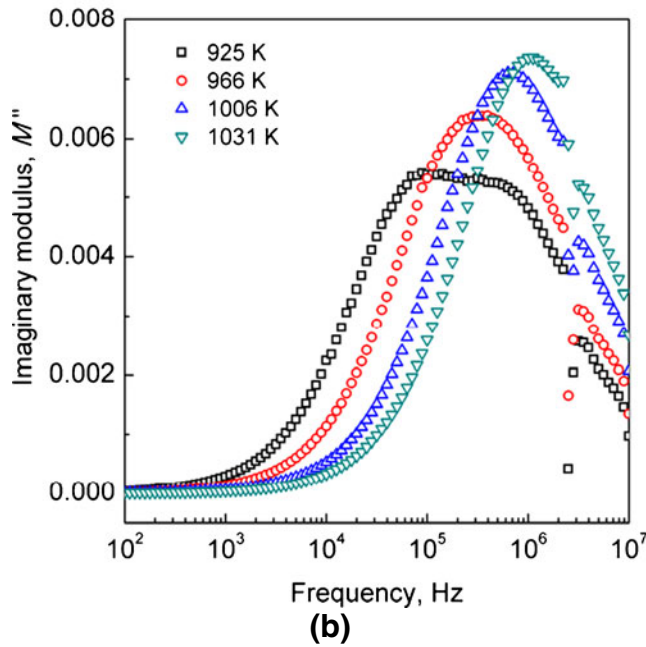
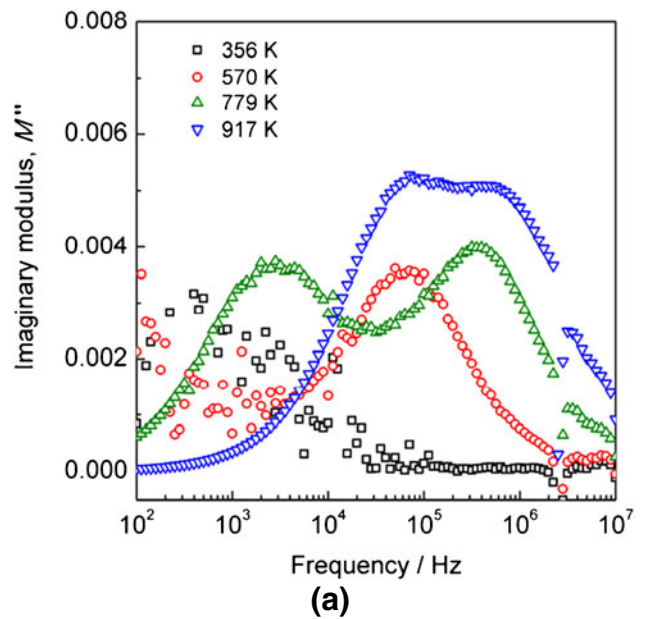


**Fig. 3** Frequency dependence of the imaginary part ( $M''$ ) of electric modulus at different temperatures: (a) from 356 to 917 K and (b) from 925 to 1031 K

Figure 4 shows the ac electrical conductivity plots as a function of frequency of Ba<sub>4</sub>Ti<sub>13</sub>O<sub>30</sub> film at different temperatures. The curves tended to flatten with increasing temperature, especially at the low-frequency regions, which was associated with dc electrical conduction. Below 876 K, as frequency increased, the step-like curves were observed due to two dispersion regions. The low-frequency dispersion was associated with grain boundaries and the high-frequency one corresponded to

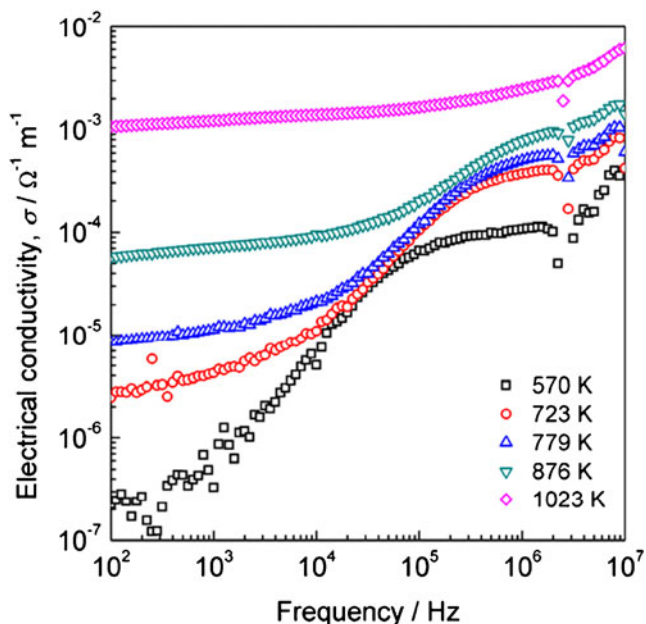
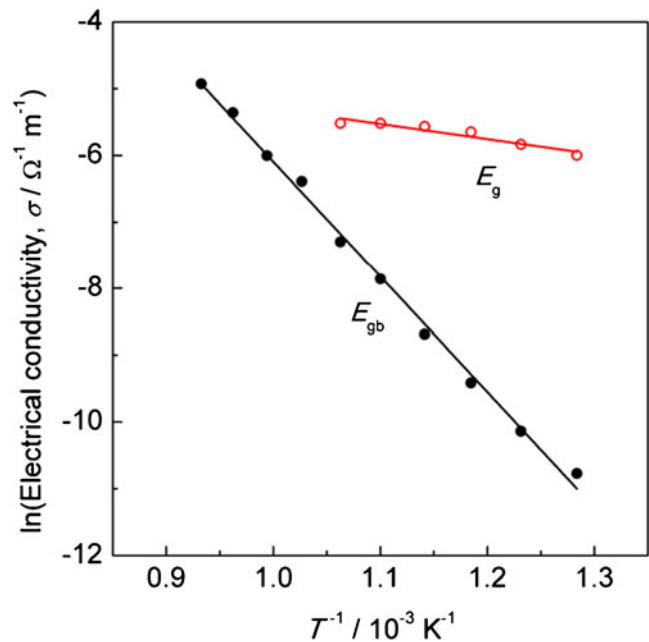
**Table 1** The calculated parameters of Ba<sub>4</sub>Ti<sub>13</sub>O<sub>30</sub> film at different temperatures

T (K)	$f_{\max I}$ (Hz)	$C_g$ (nF)	$R_g$ ( $\Omega$ )	$f_{\max II}$ (Hz)	$C_{gb}$ (nF)	$R_{gb}$ ( $\Omega$ )
779	354813	1.11	403	2818	1.18	47712
812	446684	1.04	342	5623	1.12	25254
844	562341	1.00	283	12589	1.03	12251
876	630957	0.97	261	28184	0.95	5957
909	707946	0.90	249	70794	0.87	2595
941	794328	0.80	249	141254	0.76	1474

grains [14]. When temperature was above 876 K, only one dispersion was observed due to grain boundaries and the frequency-independent behavior of dc conduction became dominant. The Arrhenius plots of the grain and grain boundary conductance are shown in Fig. 5. The electrical conductivity ( $\sigma$ ) of the grain and grain boundary had a linear relationship with temperature in Arrhenius format. The Arrhenius equation was given by

$$\sigma = \sigma_0 \exp(-E_a/kT) \quad (5)$$

where  $\sigma_0$  is a preexponential factor,  $E_a$  the activation energy of conduction,  $k$  the Boltzmann constant and  $T$  the absolute temperature. The  $E_a$  of grain ( $E_g$ ) and grain boundary ( $E_{gb}$ ) were 0.20 and 1.49 eV, respectively, which indicated that the relaxation process in grains arose from hopping electron and that in grain boundaries from the diffusion of oxygen vacancies [15].

**Fig. 4** Frequency dependence of ac electrical conductivity of Ba<sub>4</sub>Ti<sub>13</sub>O<sub>30</sub> film**Fig. 5** Arrhenius plots of grain and grain boundary conductance for Ba<sub>4</sub>Ti<sub>13</sub>O<sub>30</sub> film

#### 4 Conclusions

The impedance response of Ba<sub>4</sub>Ti<sub>13</sub>O<sub>30</sub> film was resolved into two contributions, which were associated with the grains and grain boundaries. With increasing temperature, both  $R$  and  $C$  decreased.  $R_{gb}$  was much higher than  $R_g$  and  $C_g$  were close to  $C_{gb}$ . Below 876 K, a step-like behavior was observed in the ac electrical conductivity plots as functions of frequency due to two dispersion regions. The low-frequency dispersion was associated with grain boundaries and the high-frequency one corresponded to grains. The  $E_g$  and  $E_{gb}$  were 0.20 and 1.49 eV, respectively, which indicated that the relaxation process in grains arose from hopping electron and that in grain boundaries from the diffusion of oxygen vacancies.

**Acknowledgement** This work was supported in part by Global COE Program of the Materials Integration, Tohoku University, and by the International Science and Technology Cooperation Program of China (Grant No. 2009DFB50470).

#### Reference

1. H.M. O'Bryan, J. Thomson, J.K. Plourde, J. Am. Ceram. Soc. **57**, 450 (1974)
2. L.M.B. Alldredge, W. Chang, S.W. Kirchoefer, J.M. Pond, Appl. Phys. Lett. **95**, 222902 (2009)
3. T. Negas, R.S. Roth, H.S. Papker, D. Minor, J. Solid State Chem. **9**, 297 (1974)
4. D.E. Rase, R. Roy, J. Am. Ceram. Soc. **38**, 102 (1955)
5. K.W. Kirby, B.A. Wechsler, J. Am. Ceram. Soc. **74**, 1841 (1991)
6. Y. Naki, S. Fukuoka, Jpn. J. Appl. Phys. **38**, 5568 (1999)

7. D.Y. Guo, T. Goto, C.B. Wang, Q. Shen, L.M. Zhang, J. Mater. Sci. **47**, 1559 (2012)
8. A.R. West, D.C. Sinclair, N. Hirose, J. Electroceram. **1**, 65 (1997)
9. N. Hirose, A.R. West, J. Am. Ceram. Soc. **79**, 1633 (1996)
10. D.C. Sinclair, A.R. West, Phys. Rev. B **39**, 13486 (1989)
11. A. Srivastava, A. Garg, F.D. Morrison, J. Appl. Phys. **105**, 054103 (2009)
12. T.B. Adams, D.C. Sinclair, A.R. West, Phys. Rev. B **73**, 094124 (2006)
13. J.R. Macdonald, Ann. Biomed. Eng. **20**, 289 (1992)
14. F. Salam, J.C. Giuntini, S.S. Soulayman, J.V. Zanchetta, Appl. Phys. A **63**, 447 (1996)
15. Q. Ke, X. Lou, Y. Wang, J. Wang, Phys. Rev. B **82**, 024102 (2010)